Vehicle Actuator Fault Detection With Finite-Frequency Specifications via Takagi-Sugeno Fuzzy Observers: Theory and Experiments

Juntao Pan, Tran Anh-Tu Nguyen, Thierry-Marie Guerra, Chouki Sentouh, Sujun Wang, Jean-Christophe Popieul

Vehicle Actuator Fault Detection With Finite-Frequency Specifications via Takagi-Sugeno Fuzzy Observers: Theory and Experiments

Article *in* IEEE Transactions on Vehicular Technology · September 2022

DOI: 10.1109/TVT.2022.3204326

CITATIONS
9

READS
273

6 authors, including:

Anh-Tu Nguyen
Université Polytechnique Hauts-de-France
140 PUBLICATIONS **2,084** CITATIONS
SEE PROFILE

Thierry-Marie Guerra
Université Polytechnique Hauts-de-France
349 PUBLICATIONS **9,873** CITATIONS
SEE PROFILE

Chouki Sentouh
LAMIH UMR CNRS 8201 Hauts-de-France Polytechnic University
114 PUBLICATIONS **2,057** CITATIONS
SEE PROFILE

J.-C. Popieul
Université Polytechnique Hauts-de-France
61 PUBLICATIONS **439** CITATIONS
SEE PROFILE

Vehicle Actuator Fault Detection with Finite-Frequency Specifications via Takagi-Sugeno Fuzzy Observers: Theory and Experiments

Juntao Pan, Anh-Tu Nguyen*, *Senior Member, IEEE*, Thierry-Marie Guerra, Chouki Sentouh, Sujun Wang, Jean-Christophe Popieul

***Abstract*—This paper presents a new nonlinear observer-based method to detect the faults of both steering and torque actuators of autonomous ground vehicles. To this end, the nonlinear vehicle system is reformulated in a Takagi-Sugeno (TS) fuzzy model with both measured and unmeasured nonlinear consequents, called N-TS fuzzy model. Differently from the classical TS fuzzy technique with linear consequents, this N-TS fuzzy reformulation enables an effective use of differential mean value theorem to deal with unmeasured nonlinearities, which is known as a major challenge in TS fuzzy observer design. Moreover, the N-TS fuzzy form also allows reducing not only the design conservatism but also the numerical complexity of the design conditions as well as the observer structure, which is crucial for real-time vehicle application. To minimize the disturbance effect with an $\mathscr{H}_\infty$ performance and maximize the fault sensibility with an $\mathscr{H}_-$ performance, the *a priori* information on the disturbance/fault frequency ranges is taken into account in the N-TS fuzzy observer design via the generalized Kalman–Yakubovich–Popov (KYP) lemma. Based on Lyapunov stability theory, the design of the proposed multiobjective $\mathscr{H}_-/\mathscr{H}_\infty$ N-TS fuzzy fault detector is recast as an optimization problem with strict linear matrix inequality (LMI) constraints, which can be effectively solved with numerical solvers. Both numerical and experiments are performed under realistic driving conditions to demonstrate the theoretical and practical interests of the new finite-frequency fuzzy fault detection method.**

***Index Terms*—Vehicle dynamics and estimation, Takagi-Sugeno fuzzy model, fault detection, linear matrix inequality, mixed $\mathscr{H}_-/\mathscr{H}_\infty$ performance, steering faults.**

I. Introduction

AUTONOMOUS vehicles (AVs), which are expected to improve the passenger safety and the road traffic efficiency, have received increasing attention over the last decades [1]–[7]. In particular, many research efforts have been devoted to the safety issues of AVs [8]–[10]. The vehicle active safety systems, such as lane keeping system, electronic stability control system, antilock braking system, traction control system, etc., are critical to the safety of AVs. The operation of these systems significantly relies on the accurate information of vehicle onboard signals [11]–[14]. Unfortunately, many factors, *e.g.*, circuit aging and malfunction, may cause unexpected actuator and/or sensor faults which can lead to a serious performance degradation of active safety systems. Hence, developing fault detection (FD), fault diagnosis and fault-tolerant control strategies to avoid negative impacts of actuator and sensor faults is crucial research topics for AVs, see for instance [10], [15]–[19] and related references.

Hardware redundancy and analytical redundancy have been considered for FD strategies to improve the system reliability [20]. However, due to cost reasons, it is not realistic to equip hardware redundancy to the whole system. Hence, analytical redundancy approaches have become the mainstream for FD research topic [21], which can be categorized into signal-based methods, knowledge-based methods and model-based methods. Using extracted features from measured signals, the FD performance of signal-based methods can be greatly degraded in the presence of unknown disturbances. Requiring a large amount of training data, knowledge-based methods can suffer high computational costs and the FD performance strongly depends on the quality of collected data [22]. Differently from these model-free methods, model-based FD algorithms can be easily onboard implemented and only require a reasonable amount of real-time data. Hence, model-based FD methods have been extensively studied in the literature [20], [21], [23].

Model-based fault detection is based on a consistency check of the residual signal, defined as the difference between the measured signal and the observer output [23], [24]. To achieve a satisfactory FD performance, the design observer should have the best robustness to the unknown disturbance and the best sensitivity to the fault signal. To this end, FD observers satisfying the well-known $\mathscr{H}_-/\mathscr{H}_\infty$ performance have been developed, see [21], [25]–[27] and related references. It is important to note that for many engineering applications, *e.g.*, autonomous vehicles, the *a priori* information on the frequency domains of the system disturbances and faults

This work is supported in part by the French Ministry of Higher Education and Research, in part by the National Center for Scientific Research (CNRS), in part by the ANR CoCoVeIA project (ANR-19-CE22-0009), in part by the ANR HM-Science project (ANR-21-CE48-0021), in part by the Nord-Pas-de-Calais Region under the project ELSAT 2020, in part by the National Natural Science Foundation of China under Grant 62163002, in part by the Natural Science Foundation of Ningxia Hui Autonomous Region under Grant 2021AAC05011, in part by the Major Special Project of North Minzu University under Grant ZDZX201902, in part by the Advanced Intelligent Perception and Control Technology Innovative Team of Ningxia.

J. Pan and S. Wang are with the School of Electrical and Information Engineering, North Minzu University, Yinchuan, China 750021. This work was partially done during the six-month stay of Dr. Pan at LAMIH laboratory. Email: jtpan@aliyun.com, sujunwang@aliyun.com.

A.-T. Nguyen, C. Sentouh and J.-C. Popieul are with LAMIH laboratory UMR CNRS 8201, Université Polytechnique Hauts-de-France, and also with INSA Hauts-de-France, 59300 Valenciennes, France. Email: tnguyen,chouki.sentouh,jean-christophe.popieul@uphf.fr.

T.-M. Guerra is with LAMIH laboratory UMR CNRS 8201, Université Polytechnique Hauts-de-France, F-59313 Valenciennes, France. Email: guerra@uphf.fr.

*Corresponding author (e-mail: nguyen.trananhtu@gmail.com).

can be available. For instance, the external disturbances and measurement noises of Radar tracking are mainly located in middle and low frequency ranges [28]. The vehicle steering angle generally has a low-frequency working range [29], [30]. Therefore, taking into account the finite-frequency information of disturbances/faults into the design of FD observers or fault estimation methods can lead to less conservative results, *i.e.*, a better FD or fault estimation performance, compared to full-frequency methods, for which frequency characteristics of signals are neglected [26], [31]. In particular, $\mathscr{H}_-$ design of full-frequency FD observers has been only valid when the sensor fault distribution matrix verifies a full column-rank condition [25]. Then, when only actuator faults are considered, as the case of this paper, full-frequency FD observer design methods usually lead to a zero $\mathscr{H}_-$ index, which is not useful to improve the fault sensitivity performance [32]. Based on the generalized Kalman–Yakubovich–Popov (KYP) lemma [33], numerous results on finite-frequency FD observer design and robust fault estimation have been developed. Finite-frequency $\mathscr{H}_-/\mathscr{H}_\infty$ fault detection has been investigated for linear systems [27], linear parameter-varying descriptor systems [34], Takagi-Sugeno (TS) fuzzy systems [35], [36], Lipschitz nonlinear systems [26], etc. A robust finite-frequency $\mathscr{H}_\infty$ fault estimation method has been proposed in [31], in which the TS fuzzy system is extended to include the fault vector in the extended system state. The control and observer design in finite-frequency domains has been successfully applied to various real-world applications [28], [29], [37], [38]. However, most of the existing results are related to linear systems or systems with measurable nonlinearities, which can be very restrictive from the practical viewpoint. To overcome this drawback, a finite-frequency $\mathscr{H}_-/\mathscr{H}_\infty$ fault detection method for discrete-time TS fuzzy systems with unmeasurable premise variables has been recently proposed in [32]. Unfortunately, based on the well-known Lipschitz property of the membership functions (MFs) to deal with the major issue of unmeasured premise variables, this method can lead to over-conservative design results, especially when the Lipschitz constant of nonlinear systems is large [39].

Motivated by the above discussions, we develop a novel nonlinear fault detector for both steering and longitudinal torque actuators of AVs. Note that only steering actuator fault detection can be achieved in [29]. Due to the nonlinear nature of the vehicle system in our application, TS fuzzy technique is used for FD observer design. Differently from the classical TS fuzzy modeling [40], [41] widely used in the literature, the nonlinear vehicle dynamics is reformulated as a specific TS fuzzy model with both measured and unmeasured nonlinear consequents, called N-TS fuzzy form. This N-TS fuzzy reformulation allows for an effective use of the differential mean value theorem to avoid the conservative Lipschitz assumption in TS fuzzy observer design [39]. Finite-frequency specifications of actuator faults as well as vehicle disturbances are taken into account via the generalized KYP lemma in the observer design to improve both the robustness and the sensibility performances of the proposed TS fuzzy fault detector. Specifically, the contributions of the paper can be summarized as follows.

1) Using N-TS fuzzy reformulation for nonlinear systems, we propose a mixed $\mathscr{H}_-/\mathscr{H}_\infty$ observer-based method for actuator fault detection of a large class of engineering systems with *unmeasured* nonlinearities. Not only the numerical complexity of the TS fuzzy observer structure and the design conditions but also the design conservatism can be significantly reduced for real-world applications.
2) Based on Lyapunov stability theory and the generalized KYP lemma, we propose a multiobjective $\mathscr{H}_-/\mathscr{H}_\infty$ N-TS fuzzy fault detection method taking into account finite-frequency specifications to minimize the disturbance effect and maximize the fault sensibility performance. The design procedure is reformulated as an optimization problem under linear matrix inequalities (LMIs), which can be effectively solved with numerical solvers.
3) We conduct both numerical and experiment tests to validate both theoretical and practical interests of the designed $\mathscr{H}_-/\mathscr{H}_\infty$ N-TS fuzzy fault detector. It is important to note that the existing results on FD and fault estimation in [26], [27], [29], [34]–[36] and references therein cannot be directly applied to the considered nonlinear vehicle system. Moreover, the recent method on finite-frequency $\mathscr{H}_-/\mathscr{H}_\infty$ fault detection in [32] cannot provide a feasible FD solution for this vehicle application due to its over-conservativeness.

Notation. Symbols $\mathbb{R}^{n\times m}$ and $\mathbb{H}^{n\times m}$ denote the set of $n\times m$ real and Hermitian matrices. The set of nonnegative integers is denoted by $\mathbb{Z}_+$ and $\mathcal{I}_{n_r}=\{1,2,\ldots,n_r\}\subset\mathbb{Z}_+$. For $i\in\mathcal{I}_{n_r}$, we denote $\sigma_{n_r}(i)=[0,\ldots,0,1_{i\text{th}},0,\ldots,0]^\top\in\mathbb{R}^{n_r}$ a vector of the canonical basis of $\mathbb{R}^{n_r}$. For a vector x, x_i denotes its ith entry. For two vectors $x,y\in\mathbb{R}^n$, the convex hull of these vectors is denoted as $\text{co}(x,y)=\{\lambda x+(1-\lambda)y:\ \lambda\in[0,1]\}$. For a matrix X, $X^\top$ denotes its transpose, $X\succ 0 (X\prec 0)$ means X is positive definite (or negative definite), and $\text{He}X=X+X^\top$. I denotes the identity matrix of appropriate dimension. In block matrices, $\star$ stands for the terms deduced by symmetry. Arguments are omitted when their meaning is clear.

II. Vehicle Modeling

Consider a two degrees-of-freedom vehicle model depicted in Fig. 1, whose nonlinear dynamics is given by [14]

$$\begin{aligned}\dot{v}_x&=\frac{T_l}{I_e}-\frac{C_x v_x^2}{M_v}+v_y\varphi\\ \dot{v}_y&=\frac{F_{yf}+F_{yr}-C_y v_y^2}{M_v}-v_x\varphi\\ \dot{\varphi}&=\frac{l_f F_{yf}-l_r F_{yr}}{I_z}+\frac{F_w}{I_z}\end{aligned}\tag{1}$$

where v_x [m/s] is the vehicle speed, v_y [m/s] is the lateral speed, φ [rad/s] is the vehicle yaw rate, and T_l [Nm] is the torque input for the longitudinal dynamics, F_w [N] represents the lateral wind force, F_{yf} and F_{yr} are respectively the cornering forces at the front and the rear tires. The vehicle parameters are given in Table I.

In real-word driving scenarios, the longitudinal speed v_x and the yaw rate φ can be measured from sensors while the

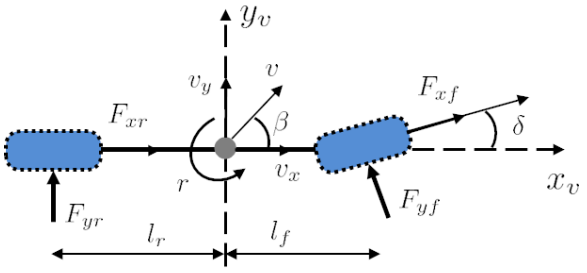

Fig. 1. Schematic of a two degrees-of-freedom vehicle model.

TABLE I
VEHICLE PARAMETERS.

Parameter	Description	Value
M_v	Vehicle mass	1476 [kg]
l_f	Distance from gravity center to front axle	1.13 [m]
l_r	Distance from gravity center to rear axle	1.49 [m]
I_e	Effective longitudinal inertia	442.8 [kgm^2]
I_z	Vehicle yaw moment of inertia	1810 [kgm^2]
C_f	Front cornering stiffness	57000 [N/rad]
C_r	Rear cornering stiffness	59000 [N/rad]
C_x	Longitudinal aerodynamic drag coefficient	0.35 [–]
C_y	Lateral aerodynamic drag coefficient	0.45 [–]

measurement of the lateral speed v_y is not available. Hence, the output equation of system (1) is given by

$$y = Cx, \quad C = \begin{bmatrix} 1 & 0 & 0 \\ 0 & 0 & 1 \end{bmatrix}. \tag{2}$$

We consider the normal driving situations with small angle assumption [42]. Then, the compact set representing the physical limitations of the vehicle state can be defined as

$$\mathscr{D}_x = \left\{ v_x \in [\underline{v}_x, \overline{v}_x],\ v_y \in [\underline{v}_y, \overline{v}_y],\ \varphi \in [\underline{\varphi}, \overline{\varphi}] \right\}.$$

where $\underline{v}_x = 5$ [m/s], $\overline{v}_x = 30$ [m/s], $\underline{v}_y = -1.5$ [m/s], $\overline{v}_y = 1.5$ [m/s], $\underline{\varphi} = -0.55$ [rad/s] and $\overline{\varphi} = 0.55$ [rad/s]. Moreover, the lateral tire forces are proportional to the slip angles of each axle, which can be approximated as follows [12]:

$$F_{yf} = 2C_f \left(\delta - \frac{v_y + l_f \varphi}{v_x} \right),\ F_{yr} = 2C_r \left(\frac{l_r \varphi - v_y}{v_x} \right), \tag{3}$$

where δ is the front-wheel steering angle. We assume that the vehicle is subject to actuator faults in both the steering system and the driving system. Then, the actual front-wheel steering angle δ and the longitudinal torque T_l can be represented as

$$\delta = \delta_d + b_\delta \delta_f, \quad T_l = T_d + b_T T_f, \tag{4}$$

where δ_d and T_d are respectively the desired front-wheel steering angle and the longitudinal torque, δ_f is the steering angle induced by the faults, T_f represents the fault related to the longitudinal torque, b_δ and b_T are the coefficients whose values depend on the gains of the actuators [29]. Inspired by the N-TS fuzzy modeling [43], the faulty vehicle model can be reformulated from (1), (3) and (4) as

$$\dot{x} = A_v(\xi)x + B_v u + F_v f + D_v w + g_v(\xi) + G_v \phi(x), \tag{5}$$

where $x = \begin{bmatrix} v_x & v_y & \varphi \end{bmatrix}^\top$ is the vehicle state vector, $u = \begin{bmatrix} T_d & \delta_d \end{bmatrix}^\top$ is the actuator input vector, $f = \begin{bmatrix} T_f & \delta_f \end{bmatrix}^\top$ is the actuator fault vector, $w = F_w$ is the external disturbance, $\phi(x) = v_y^2$ is the *unmeasured* nonlinearity. The vector of *measured* premise variables is defined as $\xi = \begin{bmatrix} \frac{1}{v_x} & \varphi \end{bmatrix}^\top$. The state-space matrices of the nonlinear vehicle model (5) are given by

$$A_v(\xi) = \begin{bmatrix} 0 & \varphi & 0 \\ 0 & -\frac{2(C_f+C_r)}{M_v v_x} & 0 \\ 0 & \frac{2(l_r C_r - C_f l_f)}{I_z v_x} & 0 \end{bmatrix}, \quad D_v = \begin{bmatrix} 0 \\ 0 \\ \frac{1}{I_z} \end{bmatrix},$$

$$g_v(\xi) = \begin{bmatrix} -\frac{C_x v_x^2}{M_v} \\ \frac{2(C_r l_r - C_f l_f)\varphi}{M_v v_x} - v_x \varphi \\ -\frac{2(C_f l_f^2 + C_r l_r^2)\varphi}{I_z v_x} \end{bmatrix}, \quad G_v = \begin{bmatrix} 0 \\ -\frac{C_y}{M_v} \\ 0 \end{bmatrix},$$

$$F_v = \begin{bmatrix} b_1 b_T & 0 \\ 0 & b_2 b_\delta \\ 0 & b_3 b_\delta \end{bmatrix}, \quad B_v = \begin{bmatrix} b_1 & 0 \\ 0 & b_2 \\ 0 & b_3 \end{bmatrix},$$

$$b_1 = \frac{1}{I_e}, \quad b_2 = \frac{2C_f}{M_v}, \quad b_3 = \frac{2 l_f C_f}{I_z}.$$

Using the explicit Euler's transformation, the discrete-time form of the nonlinear vehicle model (5) with the output vector in (2) can be obtained as

$$\begin{aligned} x_{k+1} &= A(\xi_k)x_k + F f_k + D d_k + g(\xi_k, u_k) + G\phi(x_k), \\ y_k &= Cx_k, \end{aligned} \tag{6}$$

with

$$\begin{aligned} A(\xi_k) &= T_s A_v(\xi_k) + I, \quad B = T_s B_v, \quad F = T_s F_v, \\ g(\xi_k, u_k) &= T_s g_v(\xi_k) + B u_k, \quad G = T_s G_v, \quad D = T_s D_v, \end{aligned}$$

and $T_s = 0.01$ [s] is the sampling time. Applying the sector nonlinearity approach [40] to system (6) with two measured premise variables $\varrho_x = \frac{1}{v_x} \in [\underline{\varrho}_x, \overline{\varrho}_x]$ and $\varphi \in [\underline{\varphi}, \overline{\varphi}]$, the following four-rule N-TS fuzzy model can be derived:

$$\begin{aligned} x_{k+1} &= A(h)x_k + F f_k + D d_k + g(\xi_k, u_k) + G\phi(x_k), \\ y_k &= Cx_k, \end{aligned} \tag{7}$$

where $A(h) = \sum_{i=1}^{4} h_i(\xi_k) A_i$, $A_i = A(h)|_{h_i(\xi_k)=1}$, and

$$\begin{aligned} h_1(\xi) &= \varpi_{\varrho_1} \varpi_{\varphi_1}, \quad h_2(\xi) = \varpi_{\varrho_1} \varpi_{\varphi_2}, \\ h_3(\xi) &= \varpi_{\varrho_2} \varpi_{\varphi_1}, \quad h_4(\xi) = \varpi_{\varrho_1} \varpi_{\varphi_1}, \end{aligned}$$

with

$$\begin{aligned} \varpi_{\varrho_1} &= \frac{\overline{\varrho}_x - \varrho_x}{\overline{\varrho}_x - \underline{\varrho}_x}, \quad \varpi_{\varphi_1} = \frac{\overline{\varphi} - \varphi}{\overline{\varphi} - \underline{\varphi}}, \\ \varpi_{\varrho_2} &= \frac{\varrho_x - \underline{\varrho}_x}{\overline{\varrho}_x - \underline{\varrho}_x}, \quad \varpi_{\varphi_2} = \frac{\varphi - \underline{\varphi}}{\overline{\varphi} - \underline{\varphi}}. \end{aligned}$$

III. FUZZY OBSERVER DESIGN WITH FINITE-FREQUENCY SPECIFICATIONS FOR FAULT DETECTION

This section presents a new framework to design nonlinear FD observers for a class of N-TS fuzzy systems. To improve the FD performance, the frequency information of faults is taken into account in the TS fuzzy observer design.

A. Observer Structure and Problem Formulation

For generality, we consider the N-TS fuzzy model (7) in a more general form

$$\begin{aligned} x_{k+1} &= A(h)x_k + g(\xi_k, u_k) + G(h)\phi(x_k) + Dd_k + Ff_k, \\ y_k &= Cx_k, \end{aligned} \tag{8}$$

where $x_k \in \mathscr{D}_x \subseteq \mathbb{R}^{n_x}$ is the system state, $u_k \in \mathbb{R}^{n_u}$ is the known input, $y_k \in \mathbb{R}^{n_y}$ is the system output, $d_k \in \mathbb{R}^{n_w}$ is the unknown disturbance, $f_k \in \mathbb{R}^{n_f}$ is the unknown actuator fault, $\xi_k \in \mathbb{R}^{n_\xi}$ is the vector of measured premise variables. Assume that the frequency ranges of $d_k \in l_2[0,\infty)$ and $f_k \in l_2[0,\infty)$ are finite and known in advance. The state-space matrices of system (8) are given by

$$A(h) = \sum_{i=1}^{n_r} h_i(\xi_k)A_i, \quad G(h) = \sum_{i=1}^{n_r} h_i(\xi_k)G_i.$$

Note that the MFs satisfy the following convex sum property:

$$\sum_{i=1}^{n_r} h_i(\xi_k) = 1, \quad 0 \le h_i(\xi_k) \le 1, \quad \forall i \in \mathcal{I}_{n_r}. \tag{9}$$

Let $\mathscr{H}$ be the set of membership functions satisfying (9), *i.e.*, $h = \left[h_1(\xi_k), h_2(\xi_k), \ldots, h_{n_r}(\xi_k)\right]^\top \in \mathscr{H}$. We also denote $h_+ = \left[h_1(\xi_{k+1}), h_2(\xi_{k+1}), \ldots, h_{n_r}(\xi_{k+1})\right]^\top \in \mathscr{H}$. We consider the following assumption for system (8).

Assumption 1. The nonlinear function $\phi : \mathscr{D}_x \to \mathbb{R}^{n_\phi}$ is differentiable with respect to x_k, and satisfies the condition

$$\underline{\rho}_{ij} \le \frac{\partial \phi_i}{\partial x_j}(x) \le \overline{\rho}_{ij}, \qquad x \in \mathscr{D}_x, \tag{10}$$

where $\underline{\rho}_{ij} = \min\limits_{\mu \in \mathscr{D}_x} \left(\frac{\partial \phi_i}{\partial x_j}(\mu)\right)$, $\overline{\rho}_{ij} = \max\limits_{\mu \in \mathscr{D}_x} \left(\frac{\partial \phi_i}{\partial x_j}(\mu)\right)$, for $\forall (i,j) \in \mathcal{I}_{n_\phi} \times \mathcal{I}_{n_x}$.

Remark 1. The boundedness assumption in (10) is not restrictive for N-TS fuzzy observer design. Indeed, the state x_k of engineering systems is always physically bounded, *i.e.*, $x_k \in \mathscr{D}_x$. Then, for a nonlinear system, its N-TS fuzzy representation is generally defined within $\mathscr{D}_x$, especially when using the sector nonlinear approach [40, Chapter 2]. Moreover, the bounds $\underline{\rho}_{ij}$ and $\overline{\rho}_{ij}$, for $\forall (i,j) \in \mathcal{I}_{n_\phi} \times \mathcal{I}_{n_x}$, in (10) can be easily computed from the mathematical expression of $\phi(x)$. In the sequel, Assumption 1 is useful to deal with this *unmeasured* nonlinear consequent $\phi(x)$ via the differential mean value theorem when designing N-TS fuzzy observers.

Motivated by unknown input observer structures [44], we consider the following TS fuzzy observer for fault detection:

$$\begin{aligned} z_{k+1} &= N(h)z_k + L(h)y_k + Mg(\xi_k, u_k) + MG(h)\phi(\hat{x}_k) \\ \hat{x}_k &= z_k - Ey_k \\ \hat{y}_k &= C\hat{x}_k \end{aligned} \tag{11}$$

where z_k is the observer state, $\hat{x}_k$ is the estimate of x_k. The matrices $N(h) \in \mathbb{R}^{n_x \times n_x}$, $L(h) \in \mathbb{R}^{n_x \times n_y}$, $M \in \mathbb{R}^{n_x \times n_x}$ and $E \in \mathbb{R}^{n_x \times n_y}$ are to be determined with

$$N(h) = \sum_{i=1}^{n_r} h_i(\xi_k)N_i, \quad L(h) = \sum_{i=1}^{n_r} h_i(\xi_k)L_i.$$

Moreover, these designed matrices satisfy the conditions

$$M = I + EC, \tag{12}$$

$$MA(h) - N(h)M - L(h)C = 0. \tag{13}$$

Let us define the estimation error as $e_k = x_k - \hat{x}_k$ and the residual signal as $r_k = y_k - \hat{y}_k$. Then, it follows from (11) and (12) that

$$\begin{aligned} e_k &= Mx_k - z_k, \\ r_k &= Ce_k. \end{aligned} \tag{14}$$

From (8), (11), (13) and (14), the estimation error dynamics can be defined as

$$e_{k+1} = N(h)e_k + MG(h)\delta_k + MDd_k + MFf_k, \tag{15}$$

where $\delta_k = \phi(x_k) - \phi(\hat{x}_k)$. Note that the mismatch term δ_k in (15) which caused by the unmeasured nonlinearities raises major challenge in TS fuzzy observer design [39]. To effectively deal with this term and guarantee an asymptotic error convergence, the following differential mean value theorem is introduced to reformulate the term $\delta_k = \phi(x_k) - \phi(\hat{x}_k)$ into a function of the estimation error e_k.

Lemma 1 ([45])**.** Let $\ell(x) : \mathbb{R}^{n_x} \to \mathbb{R}^q$ is a differentiable function on $\mathrm{co}(\alpha, \beta)$, with $\alpha, \beta \in \mathbb{R}^{n_x}$. There exist constant vectors $\gamma_i \in \mathrm{co}(\alpha, \beta)$, $\gamma_i \neq \alpha$, $\gamma_i \neq \beta$, for $\forall i \in \mathcal{I}_q$, such that

$$\ell(\alpha) - \ell(\beta) = \left(\sum_{i=1}^{q} \sum_{j=1}^{n_x} \sigma_q(i)\sigma_{n_x}^\top(j) \frac{\partial \ell_i}{\partial x_j}(\gamma_i) \right) (\alpha - \beta).$$

Applying Lemma 1 to the nonlinear function $\phi(x_k)$, then $\delta_k = \phi(x_k) - \phi(\hat{x}_k)$ can be rewritten as

$$\delta_k = \left(\sum_{i=1}^{n_\phi} \sum_{j=1}^{n_x} \sigma_{n_\phi}(i)\sigma_{n_x}^\top(j) \frac{\partial \phi_i}{\partial x_j}(\varsigma_i) \right) (x_k - \hat{x}_k). \tag{16}$$

where $\varsigma_i \in \mathrm{co}(x_k, \hat{x}_k)$, $i \in \mathcal{I}_{n_\phi}$. Denote $\rho_{ij} = \frac{\partial \phi_i}{\partial x_j}(\varsigma_i)$, for $\forall (i,j) \in \mathcal{I}_{n_\phi} \times \mathcal{I}_{n_x}$, and $\rho = \left[\rho_{11}, \ldots, \rho_{1n_x}, \ldots, \rho_{n_\phi n_x}\right]$. Due to condition (10), the parameter ρ belongs to a bounded convex set $\mathscr{S}_\phi$, whose set of $2^{n_\phi n_x}$ vertices is given by

$$\mathscr{V}_\phi = \{\rho \doteq \left[\rho_{11}, \ldots, \rho_{1n_x}, \ldots, \rho_{n_\phi n_x}\right] : \ \rho_{ij} \in [\underline{\theta}_{ij}, \overline{\theta}_{ij}]\}.$$

From (15) and (16), the error dynamics can be rewritten as

$$\begin{aligned} e_{k+1} &= \mathscr{N}(h, \rho)e_k + MDd_k + MFf_k, \\ r_k &= Ce_k, \end{aligned} \tag{17}$$

with $\mathscr{N}(h, \rho) = \sum_{i=1}^{n_r} h_i(\xi_k)\mathscr{N}_i(\rho_{lj})$ and

$$\mathscr{N}_i(\rho_{lj}) = N_i + MG_i \sum_{l=1}^{n_\phi} \sum_{j=1}^{n_x} \sigma_{n_\phi}(l)\sigma_{n_x}^\top(j)\rho_{lj}.$$

We consider the following fault detection problem.

Problem 1. Consider the nonlinear system (8) where the frequencies of $d_k \in l_2[0,\infty)$ and $f_k \in l_2[0,\infty)$ belong to a predefined interval ranges. Determine the gain matrices $N(h)$, $L(h)$, M and E of the TS fuzzy observer (11) such that

(P1) When $d_k = 0$ and $f_k = 0$, for $k \in \mathbb{Z}_+$, the estimation error dynamics (15) is internally stable.

(P2) When $f_k = 0$, for $k \in \mathbb{Z}_+$, system (15) verifies an $\mathscr{H}_\infty$ performance from d_k to r_k, *i.e.*, $\|r_k\|_2^2 < \gamma^2 \|d_k\|_2^2$, for $\gamma > 0$, in a finite-frequency domain.

(P3) When $d_k = 0$, for $k \in \mathbb{Z}_+$, system (15) verifies an $\mathscr{H}_-$ performance from f_k to r_k, *i.e.*, $\|r_k\|_2^2 > \beta^2 \|d_k\|_2^2$, for $\beta > 0$, in a finite-frequency domain.

Our goal is to design a mixed $\mathscr{H}_-/\mathscr{H}_\infty$ fault detection observer (11) to minimize γ and maximize β, *i.e.*, an observer which has the best possible robustness to d_k and the best possible sensitivity to f_k. Moreover, the frequency characteristics of both d_k and f_k are taken into account in the observer design to improve the fault detection performance. The following generalized KYP lemma is useful for this multiobjective FD observer design.

Lemma 2 (Extended from [33])**.** Consider the following discrete-time TS fuzzy system:

$$\begin{aligned} e_{k+1} &= \mathcal{A}(h)e_k + \mathcal{B}(h)\nu_k, \\ r_k &= \mathcal{C}(h)e_k + \mathcal{D}(h)\nu_k, \end{aligned} \tag{18}$$

where $\Pi(h) = \sum_{i=1}^{n_r} h_i(\xi_k)\Pi_i$, for $\Pi \in \{\mathcal{A}, \mathcal{B}, \mathcal{C}, \mathcal{D}\}$, and ν_k represents the disturbance d_k or the fault f_k. Let γ and β be two predefined positive scalars, system (18) satisfies a finite-frequency $\mathscr{H}_\infty$ performance gain γ (respectively $\mathscr{H}_-$ performance gain β) if there exist symmetric matrices $P_{wi} \in \mathbb{H}^{n_x \times n_x}$, $P_{fi} \in \mathbb{H}^{n_x \times n_x}$, for $i \in \mathcal{I}_{n_r}$, $Q \in \mathbb{H}^{n_x \times n_x}$, with $Q \succ 0$, such that condition (19) (respectively (20)) is verified

$$\Phi^\top \mathscr{P}_w \Phi + \Psi^\top \Pi_w \Psi \prec 0, \tag{19}$$

$$\Phi^\top \mathscr{P}_f \Phi + \Psi^\top \Pi_f \Psi \prec 0, \tag{20}$$

where $\Pi_w = \mathrm{diag}(I, -\gamma^2 I)$, $\Pi_f = \mathrm{diag}(-I, \beta^2 I)$, and

$$\Phi = \begin{bmatrix} \mathcal{A}(h) & \mathcal{B}(h) \\ I & 0 \end{bmatrix}, \quad \Psi = \begin{bmatrix} \mathcal{C}(h) & \mathcal{D}(h) \\ 0 & I \end{bmatrix}.$$

The expression of $\mathscr{P}$, with $\mathscr{P} \in \{\mathscr{P}_w, \mathscr{P}_f\}$, for different frequency ranges is defined in Table II with $\vartheta_c = (\vartheta_2 + \vartheta_1)/2$, $\vartheta_m = (\vartheta_2 - \vartheta_1)/2$, $P(h) = \sum_i^{n_r} h_i(\xi_k) P_i$ and $P(h_+) = \sum_i^{n_r} h_i(\xi_{k+1}) P_i$, for $P \in \{P_w, P_f\}$. Note that ω denotes the frequency of the disturbance/fault signal ν_k, and the given values ϑ_1, ϑ_2, ϑ_l and ϑ_h define the frequency ranges.

TABLE II
EXPRESSION OF $\mathscr{P}$ FOR DIFFERENT FREQUENCY RANGES.

Frequency range	$\mathscr{P}$
Low freq. $\lvert\omega\rvert \le \vartheta_l$	$\begin{bmatrix} P(h_+) & Q \\ Q & -P(h) - 2\cos(\vartheta_l)Q \end{bmatrix}$
Middle freq. $\vartheta_1 \le \omega \le \vartheta_2$	$\begin{bmatrix} P(h_+) & e^{j\vartheta_c}Q \\ e^{-j\vartheta_c}Q & -P(h) - 2\cos(\vartheta_m)Q \end{bmatrix}$
High freq. $\lvert\omega\rvert \ge \vartheta_h$	$\begin{bmatrix} P(h_+) & -Q \\ -Q & -P(h) + 2\cos(\vartheta_h)Q \end{bmatrix}$

Remark 2. Note that by setting $Q = 0$ in $\mathscr{P}$, for $\mathscr{P} \in \{\mathscr{P}_w, \mathscr{P}_f\}$, the full-frequency $\mathscr{H}_\infty$ condition (respectively $\mathscr{H}_-$ condition) can be directly recovered from (19) (respectively (20)), see [21]. Then, finite-frequency specifications offers more flexibility to the FD observer design than the standard full-frequency one. Note also that $|\omega| \le \vartheta_l$ and $|\theta| \ge \vartheta_h$ are the special cases of $\vartheta_1 \le \theta \le \vartheta_2$ by setting $-\vartheta_1 = \vartheta_2 = \vartheta_l$ and $\vartheta_1 = \vartheta_h$, $\vartheta_2 = \pi - \vartheta_h$, respectively. Hence, without loss of generality, we only consider the FD observer design with a middle-frequency range specification in the following.

B. Finite-Frequency Fault Detection Observer Design

Hereafter, we present three theorems to guarantee the three proprieties of system (15) stated in Problem 1.

1) Internal Stability Condition: Theorem 1 presents sufficient conditions to ensure the internal stability for system (17) when $d_k = 0$ and $f_k = 0$, for $k \in \mathbb{Z}_+$, *i.e.*,

$$e_{k+1} = \mathscr{N}(h, \rho) e_k. \tag{21}$$

Theorem 1 (Extended from [46])**.** The error system (21) is stable if there exist MFs-dependent positive definite matrix $P(h) \in \mathbb{R}^{n_x \times n_x}$ and a matrix $R \in \mathbb{R}^{n_x \times n_x}$ such that

$$\begin{bmatrix} P(h) & \star \\ R\mathscr{N}(h, \rho) & R + R^\top - P(h_+) \end{bmatrix} \succ 0, \tag{22}$$

for $h, h_+ \in \mathscr{H}$ and $\rho \in \mathscr{S}_\phi$.

Proof. Pre- and post-multiplying (22) with $\begin{bmatrix} I & -\mathscr{N}^\top(h, \rho) \end{bmatrix}$ and its transpose, it follows that

$$\mathscr{N}^\top(h, \rho) P(h_+) \mathscr{N}(h, \rho) - P(h) \prec 0. \tag{23}$$

Pre- and post-multiplying (23) with $e_k^\top$ and e_k, we obtain $\Delta V_k < 0$, where $\Delta V_k = V(e_{k+1}) - V(e_k)$ is the variation of the Lyapunov function candidate $V(e_k) = e_k^\top P(h) e_k$ along the trajectory of system (21). This concludes the proof. □

2) Disturbance Attenuation Condition: Theorem 2 presents sufficient conditions to ensure a finite-frequency $\mathscr{H}_\infty$ performance for system (17) when $f_k = 0$, for $k \in \mathbb{Z}_+$, *i.e.*,

$$\begin{aligned} e_{k+1} &= \mathscr{N}(h, \rho) e_k + MDd_k, \\ r_k &= Ce_k, \end{aligned} \tag{24}$$

where the frequency ω_w of the disturbance d_k satisfies

$$\vartheta_{w_1} \le \omega_w \le \vartheta_{w_2}, \tag{25}$$

with predefined scalars ϑ_{w_1} and ϑ_{w_2}.

Theorem 2. System (24) verifies a finite-frequency $\mathscr{H}_\infty$ performance index $\gamma > 0$, if there exist MFs-dependent matrices $Y(h) \in \mathbb{R}^{n_x \times n_x}$, $N(h) \in \mathbb{R}^{n_x \times n_x}$, $L(h) \in \mathbb{R}^{n_x \times n_y}$, a positive definite matrix $Q_w \in \mathbb{H}^{n_x \times n_x}$, matrices $R \in \mathbb{R}^{n_x \times n_x}$, $M \in \mathbb{R}^{n_x \times n_x}$ and $E \in \mathbb{R}^{n_x \times n_y}$ such that

$$\begin{bmatrix} \Sigma_{11} & \star & \star \\ \Sigma_{21} & -\gamma^2 I & \star \\ \Sigma_{31} & RMD & Y(h_+) - R - R^\top \end{bmatrix} \prec 0, \tag{26}$$

for $h, h_+ \in \mathscr{H}$, $\rho \in \mathscr{S}_\phi$, where

$$\begin{aligned} &\Sigma_{11} = \mathrm{He}\left[R\mathscr{N}(h, \rho)\right] - Y(h) - 2\cos(\vartheta_{wm})Q_w + C^\top C, \\ &\Sigma_{21} = (RMD)^\top, \quad \Sigma_{31} = R\mathscr{N}(h, \rho) + e^{j\vartheta_{wc}} Q_w - R^\top, \\ &\vartheta_{wc} = (\vartheta_{w_2} + \vartheta_{w_1})/2, \quad \vartheta_{wm} = (\vartheta_{w_2} - \vartheta_{w_1})/2. \end{aligned}$$

Proof. Pre- and post-multiplying (26) with

$$\begin{bmatrix} I & 0 & \mathscr{N}^\top(h, \rho) \\ 0 & I & D^\top M^\top \end{bmatrix}$$

and its transpose, it follows that

$$\Phi_w^\top \Xi_w \Phi_w + \Psi_w^\top \Pi_w \Psi_w \prec 0, \tag{27}$$

where $\Psi_w = \mathrm{diag}(C, I)$, $\Pi_w = \mathrm{diag}(I, -\gamma^2 I)$, and

$$\Phi_w = \begin{bmatrix} \mathscr{N}(h,\rho) & MD \\ I & 0 \end{bmatrix},$$
$$\Xi_w = \begin{bmatrix} Y(h_+) & e^{j\vartheta_{wc}} Q_w \\ e^{-j\vartheta_{wc}} Q_w & -Y(h) - 2\cos(\vartheta_{wm}) Q_w \end{bmatrix}.$$

According to relation (19) of Lemma 2, inequality (27) implies that system (24) verifies a finite-frequency $\mathscr{H}_\infty$ performance level γ. This concludes the proof. □

3) Fault Sensitivity Condition: Theorem 2 presents sufficient conditions to ensure a finite-frequency $\mathscr{H}_-$ performance for system (17) when $d_k = 0$, for $k \in \mathbb{Z}_+$, *i.e.*,

$$\begin{aligned} e_{k+1} &= \mathscr{N}(h,\rho) e_k + MF f_k, \\ r_k &= C e_k, \end{aligned} \tag{28}$$

where the frequency ω_f of the fault signal f_k satisfies

$$\vartheta_{f_1} \leq \omega_f \leq \vartheta_{f_2}, \tag{29}$$

with predefined scalars ϑ_{f_1} and ϑ_{f_2}.

Theorem 3. System (28) verifies a finite-frequency $\mathscr{H}_-$ performance index $\beta > 0$, if there exist MFs-dependent matrices $Z(h) \in \mathbb{R}^{n_x \times n_x}$, $N(h) \in \mathbb{R}^{n_x \times n_x}$, $L(h) \in \mathbb{R}^{n_x \times n_y}$, a positive definite matrix $Q_f \in \mathbb{H}^{n_x \times n_x}$, matrices $R \in \mathbb{R}^{n_x \times n_x}$, $M \in \mathbb{R}^{n_x \times n_x}$ and $E \in \mathbb{R}^{n_x \times n_y}$ such that

$$\begin{bmatrix} \Delta_{11} & \star & \star \\ \Delta_{21} & \Delta_{22} & \star \\ \Delta_{31} & RMF - R^\top F & Z(h_+) - R - R^\top \end{bmatrix} \prec 0, \tag{30}$$

for $h, h_+ \in \mathscr{H}$, $\rho \in \mathscr{S}_\phi$, where

$$\begin{aligned} \Delta_{11} &= \mathrm{He}[R\mathscr{N}(h,\rho)] - Z(h) - 2\cos(\vartheta_{fm}) Q_f - C^\top C, \\ \Delta_{21} &= (RMF)^\top + F^\top R \mathscr{N}(h,\rho), \\ \Delta_{22} &= \mathrm{He}\left[F^\top R M F\right] + \beta^2 I, \\ \Delta_{31} &= R\mathscr{N}(h,\rho) + e^{j\vartheta_{fc}} Q_f - R^\top, \\ \vartheta_{fc} &= (\vartheta_{f_2} + \vartheta_{f_1})/2, \quad \vartheta_{fm} = (\vartheta_{f_2} - \vartheta_{f_1})/2. \end{aligned}$$

Proof. Pre- and post-multiplying (30) with

$$\begin{bmatrix} I & 0 & \mathscr{N}^\top(h,\rho) \\ 0 & I & F^\top M^\top \end{bmatrix}$$

and its transpose, it follows that

$$\Phi_f^\top \Xi_f \Phi_f + \Psi_f^\top \Pi_f \Psi_f \prec 0, \tag{31}$$

where $\Psi_f = \mathrm{diag}(C, I)$, $\Pi_f = \mathrm{diag}(-I, \beta^2 I)$, and

$$\Phi_f = \begin{bmatrix} \mathscr{N}(h,\rho) & MF \\ I & 0 \end{bmatrix},$$
$$\Xi_f = \begin{bmatrix} Z(h_+) & e^{j\vartheta_{fc}} Q_f \\ e^{-j\vartheta_{fc}} Q_f & -Z(h) - 2\cos(\vartheta_{fm}) Q_f \end{bmatrix}.$$

According to relation (20) of Lemma 2, inequality (31) implies that system (28) verifies a finite-frequency $\mathscr{H}_-$ performance level β. This concludes the proof. □

C. LMI-Based Fault Detection Observer Design

Due to the nonlinear couplings between decision variables and their MFs-dependencies, Theorems 1–3 cannot be directly used for FD observer design. On the basis of these results, we derive hereafter tractable conditions to design a finite-frequency FD observer (11) for system (8).

Theorem 4. The error system (17) is internally stable and verifies an $\mathscr{H}_\infty$ performance index $\gamma > 0$ as well as an $\mathscr{H}_-$ performance index $\beta > 0$ in a specified finite-frequency domain (25) and (29), if there exist positive definite matrices $P_i \in \mathbb{R}^{n_x \times n_x}$, $Q_w \in \mathbb{H}^{n_x \times n_x}$, $Q_f \in \mathbb{H}^{n_x \times n_x}$, matrices $Y_i \in \mathbb{R}^{n_x \times n_x}$, $Z_i \in \mathbb{R}^{n_x \times n_x}$, $R \in \mathbb{R}^{n_x \times n_x}$, $S \in \mathbb{R}^{n_x \times n_y}$, $W_i \in \mathbb{R}^{n_x \times n_y}$, for $i \in \mathcal{I}_{n_r}$, positive scalars $\overline{\gamma}$ and $\overline{\beta}$, satisfying the following optimization problem:

$$\underset{(\overline{\gamma},\overline{\beta},P_i,Y_i,Z_i,W_i,Q_w,Q_f,R,S),\ i\in\mathcal{I}_N}{\text{minimize}} \quad \overline{\gamma} - \overline{\beta} \tag{32}$$

such that

$$\Upsilon_{im}(\rho_{lj}) = \begin{bmatrix} P_i & \star \\ \Upsilon_{21} & R + R^\top - P_m \end{bmatrix} \succ 0, \tag{33}$$

$$\Gamma_{im}(\rho_{lj}) = \begin{bmatrix} \Gamma_{11} & \star & \star \\ \Gamma_{21} & \Gamma_{22} & \star \\ \Gamma_{41} & \Gamma_{42} & Y_m - R - R^\top \end{bmatrix} \prec 0, \tag{34}$$

$$\Lambda_{im}(\rho_{lj}) = \begin{bmatrix} \Lambda_{11} & \star & \star \\ \Lambda_{21} & \Lambda_{22} & \star \\ \Lambda_{31} & \Lambda_{32} & Z_m - R - R^\top \end{bmatrix} \prec 0, \tag{35}$$

for $i, m \in \mathcal{I}_{n_r}$ and $\rho_{lj} \in \mathscr{V}_\phi$, $l \in \mathcal{I}_{n_\phi}$, $j \in \mathcal{I}_{n_x}$, where

$$\begin{aligned} \Upsilon_{21} &= (R + SC)\mathscr{A}_i(\rho_{lj}) - W_i C, \\ \Gamma_{11} &= \mathrm{He}\left[\Upsilon_{21}\right] - Y_i + C^\top C - 2\cos(\vartheta_{wm}) Q_\omega, \\ \Gamma_{21} &= D^\top (R + SC)^\top, \quad \Gamma_{22} = -\overline{\gamma} I, \\ \Gamma_{41} &= \Upsilon_{21} + e^{j\vartheta_{wc}} Q_w - R^\top, \quad \Gamma_{42} = (R + SC)D, \\ \Lambda_{11} &= \mathrm{He}\left[\Upsilon_{21}\right] - Z_i - C^\top C - 2\cos(\vartheta_{fm}) Q_f, \\ \Lambda_{21} &= F^\top (R + SC)^\top + F^\top \Upsilon_{21}, \\ \Lambda_{22} &= \mathrm{He}\left[F^\top (R + SC) F\right] + \overline{\beta} I, \\ \Lambda_{31} &= \Upsilon_{21} + e^{j\vartheta_{fc}} Q_f - R^\top, \\ \Lambda_{32} &= -R^\top F^\top + (R + SC)F, \\ \mathscr{A}_i(\rho_{lj}) &= A_i + G_i \sum_{l=1}^{n_\phi} \sum_{j=1}^{n_x} \sigma_{n_\phi}(l) \sigma_{n_x}^\top(j) \rho_{lj}. \end{aligned}$$

Moreover, the obtained $\mathscr{H}_\infty$ and $\mathscr{H}_-$ performance indices are given by $\gamma = \sqrt{\overline{\gamma}}$ and $\beta = \sqrt{\overline{\beta}}$, respectively.

Proof. Let us perform the following changes of variables:

$$H(h) = L(h) + N(h)E, \tag{36}$$
$$W(h) = RH(h), \tag{37}$$
$$S = RE. \tag{38}$$

It follows from (12), (13) and (36) that

$$N(h) = MA(h) - H(h)C. \tag{39}$$

Substituting expressions (37), (38) and (39) into conditions (22), (26) and (30), we respectively obtain

$$\Upsilon(h,h_+,\rho)=\sum_{i=1}^{n_r}\sum_{m=1}^{n_r}h_i(\xi_k)h_m(\xi_{k+1})\Upsilon_{im}(\rho_{lj})\succ 0, \quad (40)$$

$$\Gamma(h,h_+,\rho)=\sum_{i=1}^{n_r}\sum_{m=1}^{n_r}h_i(\xi_k)h_m(\xi_{k+1})\Gamma_{im}(\rho_{lj})\prec 0, \quad (41)$$

$$\Lambda(h,h_+,\rho)=\sum_{i=1}^{n_r}\sum_{m=1}^{n_r}h_i(\xi_k)h_m(\xi_{k+1})\Lambda_{im}(\rho_{lj})\prec 0. \quad (42)$$

Since $h, h_+ \in \mathscr{H}$ and due to the convexity property of $\mathscr{S}_\phi$, it follows that conditions (33), (34) and (35) imply the satisfaction of (40), (41) and (42), respectively. Based on the results of Theorems 1–3, we can conclude the proof. □

Note that the optimization problem (32) aims at minimizing the effect of disturbances and maximizing the fault sensitivity. The procedure to design multiobjective $\mathscr{H}_-/\mathscr{H}_\infty$ fault detection observers is summarized in Algorithm 1.

Algorithm 1 Design procedure of multiobjective FD observers

1: **Input:** nonlinear system (8) with a specified finite-frequency domains (25) and (29)
2: solve problem (32) to get R, S, W_i, for $i \in \mathcal{I}_{n_r}$
3: compute H_i from (37) as $H_i = R^{-1}W_i$, for $i \in \mathcal{I}_{n_r}$
4: compute E from (38) as $E = R^{-1}S$
5: compute M from (12)
6: compute matrices N_i, for $i \in \mathcal{I}_{n_r}$, from (39)
7: compute matrices L_i, for $i \in \mathcal{I}_{n_r}$, from (36)
8: construct matrices $L(h)$ and $N(h)$, then observer (11)
9: **Output:** multiobjective $\mathscr{H}_-/\mathscr{H}_\infty$ fuzzy observer (11)

D. Residual Evaluation and Threshold Setting

Once the FD observer is designed, different strategies for residual evaluation and threshold setting can be developed to detect whether a fault occurs [21], [23], [24]. Hereafter, we use the root mean square (RMS) norm-based evaluation function

$$\mathscr{J}_{RMS}=||r_k||_{RMS}=\sqrt{\frac{1}{\Delta T}\sum_{k=1}^{\Delta T}||r_{t+k}||^2}, \quad (43)$$

where r_k is defined in (17). The RMS function $\mathscr{J}_{RMS}$ measures the average energy of the fault signal over a predefined time window ΔT, which has been widely exploited in the literature [21]. For fault detection, a threshold value has to be defined to represent the maximum effect of the unknown disturbance d_k on the residual signal r_k in fault-free scenarios, *i.e.*, $f_k = 0$,

$$\mathscr{J}_{th}=\sup_{f_k=0}||r_k||_{RMS}. \quad (44)$$

Based on the evaluation in (43) and the threshold in (44), the decision logic for fault detection can be formulated as [25]

$$\begin{cases}\mathscr{J}_{RMS} > \mathscr{J}_{th} & \Rightarrow \text{ Fault alarm,}\\ \mathscr{J}_{RMS} \le \mathscr{J}_{th} & \Rightarrow \text{ Fault free.}\end{cases} \quad (45)$$

IV. Application to Vehicle Fault Detection: Numerical and Experiment Results

This section presents theoretical and experimental illustrations of the proposed FD observer design with FD decision logic (45) for vehicle actuator fault detection. The TS fuzzy observer design is reformulated as an LMI-based optimization problem (32), which can be effectively solved using standard numerical toolboxes, for instance YALMIP package with SDPT3 solver [47]. For illustration purposes, the design parameters are selected for solving the optimization problem (32) in Theorem 4 as follows: $\gamma = 2$, $\vartheta_{w_1} = -\frac{\pi}{15}$ and $\vartheta_{w_2} = \frac{\pi}{10}$ in (25), $\vartheta_{f_1} = -\frac{\pi}{10}$ and $\vartheta_{f_2} = \frac{\pi}{9}$ in (29). Note that the choice of the disturbance/fault frequency ranges is done, without loss of generality, to cover some practical situations as illustrated below. Solving the design conditions in Theorem 4, we can obtain the following observer gains:

$$N_1=\begin{bmatrix}-0.89 & 0.01 & -0.01\\ 0.00 & 0.93 & -1.89\\ 0.00 & -0.01 & -0.80\end{bmatrix}, \quad L_1=\begin{bmatrix}-1.69 & -0.01\\ 0.00 & -1.76\\ 0.00 & -1.56\end{bmatrix}$$

$$N_3=\begin{bmatrix}-0.89 & -0.01 & 0.01\\ 0.00 & 0.58 & -1.51\\ 0.00 & -0.04 & -0.76\end{bmatrix}, \quad L_3=\begin{bmatrix}-1.69 & 0.01\\ 0.00 & -2.14\\ 0.00 & -1.53\end{bmatrix}$$

$$M=\begin{bmatrix}-0.89 & 0.00 & 0.00\\ 0.00 & 1.00 & -2.02\\ 0.00 & 0.00 & -0.86\end{bmatrix}, \quad E=\begin{bmatrix}-1.89 & 0.00\\ 0.00 & -2.02\\ 0.00 & -1.86\end{bmatrix}$$

with $N_1 = N_2$, $N_3 = N_4$, $L_1 = L_2$ and $L_3 = L_4$.

A. Numerical Results and Comparative Study

To illustrate both practical and theoretical interests of the proposed TS fuzzy observer design, we perform a test scenario with the vehicle model (1), implemented in Matlab/Simulink. The vehicle trajectory, the time-varying speed v_x, the steering angle δ and the longitudinal torque input T_l are depicted in Fig. 2. For this test, we assume that the lateral wind force, *i.e.*, the vehicle external disturbance, corresponding to this scenario is $F_w = 800$ [N], which occurs from 10 [s] to 15 [s].

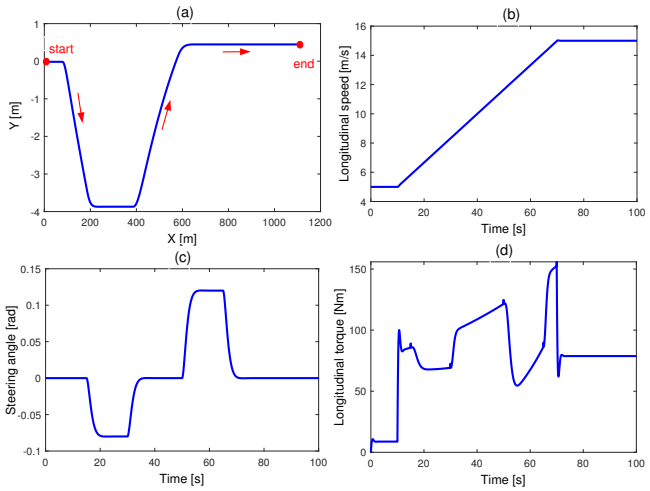

Fig. 2. Numerical test scenario. (a) Vehicle trajectory X–Y. (b) Vehicle speed v_x. (c) Steering angle δ. (d) Longitudinal torque T_l.

To validate the estimation performance, we first perform the test simulation without the presence of the fault, *i.e.*, $f_k = 0$. Fig. 3 shows the corresponding estimation results. We can see that the unmeasured lateral speed v_y can be perfectly estimated with the designed TS fuzzy observer despite the presence of the lateral wind force. To illustrate the fault detection performance, we now consider the following signals for both the steering actuator fault δ_{fk} [deg] and the torque actuator fault T_{fk} [Nm]:

$$T_{fk} = \begin{cases} 3 + \sin(0.05\pi k), & t \in \mathcal{T}_1 \\ 0, & \text{elsewhere} \end{cases}$$
$$\delta_{fk} = \begin{cases} 0.344 + 0.115\text{sawtooth}(0.14\pi k), & t \in \mathcal{T}_2 \\ 0, & \text{elsewhere} \end{cases} \quad (46)$$

where t is the simulation time in seconds, and the time sets of fault occurrence $\mathcal{T}_1$ and $\mathcal{T}_2$ are defined as

$$\mathcal{T}_1 = \{t: \ 5 \leq t \leq 40 \text{ and } 45 \leq t \leq 55\},$$
$$\mathcal{T}_2 = \{t: \ 45 \leq t \leq 55 \text{ and } 60 \leq t \leq 90\}.$$

For this test, the RMS evaluation function (43) is determined to ensure its smoothness over a moving time window of $\Delta T = 20$ [s]. For comparison purposes, we compare the fault detection performance of two TS fuzzy observers:

- Observer 1: Finite-frequency TS observer obtained from Theorem 4,
- Observer 2: Infinite-frequency TS observer obtained from Theorem 4 with $Q_w = 0$ and $Q_f = 0$, see Remark 2.

The sensibility gains obtained for both observers are respectively given by $\beta_1^\star = 0.022 > \beta_2^\star = 0.01$, meaning that Observer 1 has a better fault detection performance than Observer 2. This is also confirmed by the faut detection result depicted in Fig. 4. Note that the faults from both vehicle actuators defined in (46) can be effectively detected with the finite-frequency TS fuzzy observer, which is not the case with the other infinite-frequency observer. Indeed, as shown in Fig. 4, with Observer 2 it is not possible to detect the torque actuator fault T_{fk} occurring from 20 [s] to 40 [s]. This clearly shows the interest of taking into account the fault frequency information into the fault detection observer design. We remark that when the torque fault and the steering fault simultaneously occur from 45 [s] to 55 [s], the values of the RMS evaluation $\mathcal{J}_{RMS}$ increase for both considered TS fuzzy fault detectors. Hence, the fault occurrence can be detected more easily in this situation. It is important to note also that the recent Lipschitz-property-based approach in [32] cannot provide any feasible fault detection solution for this vehicle application due to its conservative design results. This emphasizes the practical and theoretical contributions of the proposed nonlinear fault detection method.

B. Hardware Experiments

This section presents experimental results performed with the SHERPA driving simulator. This interactive simulator is based on a Peugeot 206 mock-up fixed on a 6-axis Bosch Rexroth motion system, the overall is positioned in front of five flat panel displays providing a visual field of 240°, see Fig.

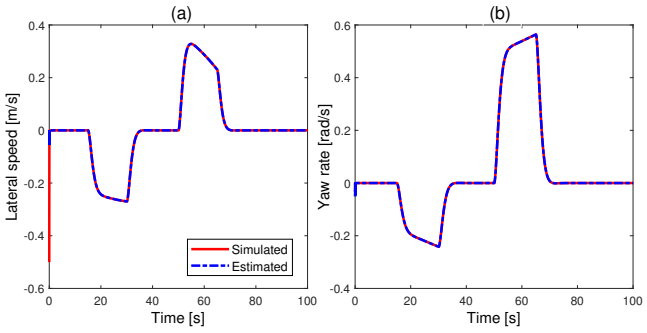

Fig. 3. Numerical state estimation. (a) Lateral speed v_y. (b) Yaw rate φ.

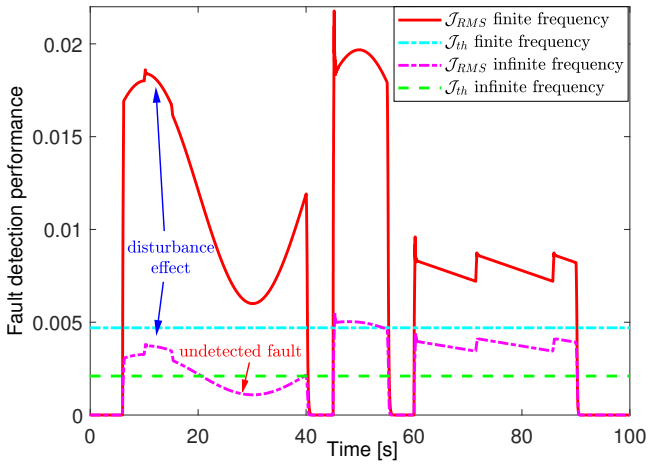

Fig. 4. Comparison of fault detection performance of finite-frequency and infinite-frequency TS fuzzy observers.

5. The simulator is equipped with a force feedback gas pedal to control the vehicle speed. The SensoDrive force feedback can provide the steering wheel torque. Moreover, the SHERPA simulator is fully instrumented to measure the vehicle dynamics [11]. Using the SCANeR™ Studio environment, the proposed TS fuzzy observer is implemented in the SHERPA simulator through Matlab/Simulink software.

To experimentally validate the proposed TS fuzzy observer, we perform a path following task with the database of the Satory test track, situated at 20km west from Paris, France, which is composed of several tight bends, see Fig. 6(a). As depicted in Fig. 6(b), the vehicle speed is highly *time-varying* and managed by a human driver during the whole test. The corresponding steering angle and longitudinal torque are shown in Figs. 6(c) and (d). For this scenario, we assume that there is no external disturbance, *i.e.*, $F_w = 0$ [N]. To evaluate the estimation performance of the proposed observer, we first consider a fault-free scenario, *i.e.*, $f_k = 0$, for $\forall k \in \mathbb{Z}_+$. Fig. 7 shows that the vehicle state variables, especially the unmeasured lateral speed v_y, can be accurately estimated via the proposed observer during the Satory test. Moreover, the following mean absolute error indicator MAE and the root mean square error indicator $RMSE$ are used to characterize

Fig. 5. SHERPA driving simulator (upper left). Steering system (upper right). Data acquisition system (bottom left). Active gas pedal (bottom right).

the estimation performance:

$$MAE = \frac{\sum_{k=1}^{\Delta_t} |s_k - \hat{s}_k|}{\Delta_t},$$
$$RMSE = \sqrt{\frac{1}{\Delta_t}\sum_{k=1}^{\Delta_t}(s_k - \hat{s}_k)^2},$$

where Δ_t is the time duration, s_k is the value of signal s at $k-$instant and $\hat{s}_k$ is its estimate. As indicated in Table III, the error indicators of the vehicle state variables are very small for the Satory test, which confirms the high-precision estimation performance of the proposed TS fuzzy observer.

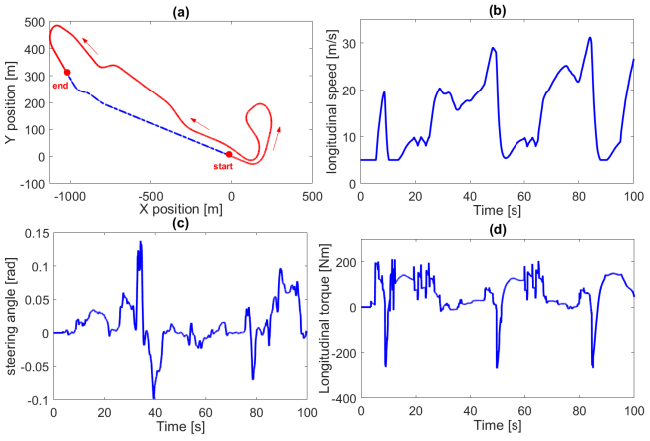

Fig. 6. Experiment test scenario. (a) Vehicle trajectory X–Y. (b) Vehicle speed v_x. (c) Steering angle δ. (d) Longitudinal torque T_l.

TABLE III
ESTIMATION PERFORMANCE INDICATOR.

Error indicator	v_x [m/s]	v_y [m/s]	φ [rad/s]
MAE	0.0164	0.0413	0.0013
$RMSE$	0.0375	0.1374	0.0027

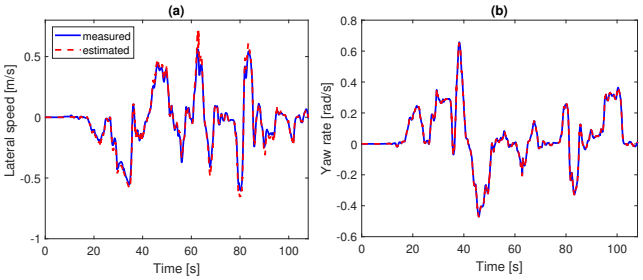

Fig. 7. Estimation performance during the Satory test. (a) Lateral speed v_y. (b) Yaw rate φ.

We now consider the same Satory driving test under a faulty-scenario, where the steering actuator fault δ_{fk} [deg] and the torque actuator fault T_{fk} [Nm] are given by

$$T_{fk} = \begin{cases} 30 + 10\sin(0.23\pi k), & t \in \mathcal{T}_3 \\ 0, & \text{elsewhere} \end{cases}$$
$$\delta_{fk} = \begin{cases} 0.5 + 0.172\sin(0.14\pi k), & t \in \mathcal{T}_4 \\ 0, & \text{elsewhere} \end{cases} \quad (47)$$

where the time sets $\mathcal{T}_3$ and $\mathcal{T}_4$ are defined as

$$\mathcal{T}_3 = \{t:\ 5 \le t \le 25 \text{ and } 55 \le t \le 65\},$$
$$\mathcal{T}_4 = \{t:\ 85 \le t \le 95\}.$$

The Satory fault detection result is depicted in Fig. 8. We can see clearly that the proposed observer-based method allows for an effective fault detection whenever the considered faults in (47) of both torque and steering actuators occur.

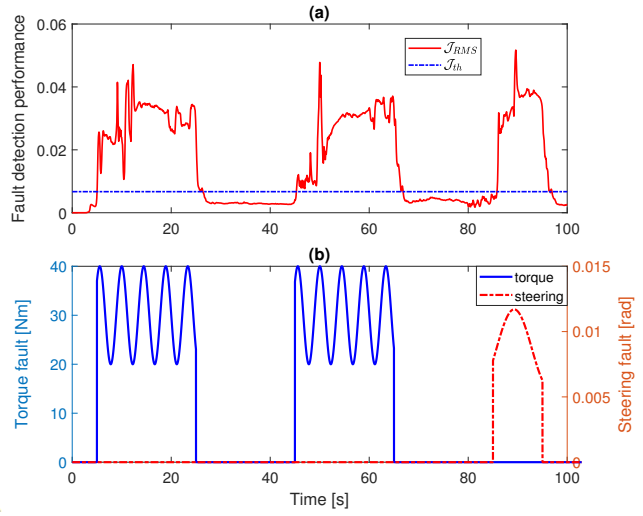

Fig. 8. Fault detection result with the Satory test track. (a) Fault detection performance. (b) Actuator fault signals.

V. CONCLUDING REMARKS

A new TS fuzzy observer-based method has been proposed for vehicle actuator fault detection. To this end, the vehicle nonlinear dynamics is represented in a N-TS fuzzy form, whose unmeasured nonlinearity is isolated in the nonlinear

consequent. This enables an effective use of the mean value theorem to deal with the challenging issue in TS fuzzy observer design in the presence of unmeasurable premise variables. To improve the fault sensitivity performance, the finite-frequency information of the disturbances and the faults is taken into account in the $\mathscr{H}_-/\mathscr{H}_\infty$ observer design via the generalized KYP lemma. Based on Lyapunov stability theory, the FD observer design is reformulated as an optimization problem under LMI constraints. Both numerical and experiment validations are performed with realistic driving conditions to demonstrate the theoretical and the practical interests of the proposed finite-frequency FD fuzzy observer. Future works focus on extending the proposed fault detection results to deal with uncertain vehicle dynamics, *e.g.*, taking into account the uncertain and/or nonlinear tire forces in the observer design to handle extreme driving conditions. Integrating the proposed N-TS fuzzy observer into a fault-tolerant control structure to achieve a robust vehicle control performance under various driving scenarios with actuator failures is another promising research topic.

REFERENCES

[1] S. Zhu, S. Gelbal, B. Aksun-Guvenc, and L. Guvenc, "Parameter-space based robust gain-scheduling design of automated vehicle lateral control," *IEEE Trans. Veh. Technol.*, vol. 68, no. 10, pp. 660–671, 2019.

[2] C. Hu, Z. Wang, H. Taghavifar, J. Na, Y. Qin, J. Guo, and C. Wei, "MME-EKF-based path-tracking control of autonomous vehicles considering input saturation," *IEEE Trans. Veh. Technol.*, vol. 68, no. 6, pp. 5246–5259, 2019.

[3] W. Zhang, Z. Wang, L. Drugge, and M. Nybacka, "Evaluating model predictive path following and yaw stability controllers for over-actuated autonomous electric vehicles," *IEEE Trans. Veh. Technol.*, vol. 69, no. 11, pp. 12 807–12 821, 2020.

[4] A.-T. Nguyen, C. Sentouh, H. Zhang, and J.-C. Popieul, "Fuzzy static output feedback control for path following of autonomous vehicles with transient performance improvements," *IEEE Trans. Intell. Transp. Syst.*, vol. 21, no. 7, pp. 3069–3079, July 2020.

[5] J. Yang, D. Zhao, J. Jiang, J. Lan, B. Mason, D. Tian, and L. Li, "A less-disturbed ecological driving strategy for connected and automated vehicles," *IEEE Trans. Intell. Vehi.*, pp. 1–1, 2021.

[6] Y. Wang, C. Wang, W. Zhao, and C. Xu, "Decision-making and planning method for autonomous vehicles based on motivation and risk assessment," *IEEE Trans. Veh. Technol.*, vol. 7, no. 1, pp. 107–120, 2021.

[7] S. Cheng, L. Li, C.-Z. Liu, X. Wu, S.-N. Fang, and J.-W. Yong, "Robust LMI-based $\mathscr{H}_\infty$ controller integrating AFS and DYC of autonomous vehicles with parametric uncertainties," *IEEE Trans. Syst., Man, Cybern.: Syst.*, vol. 51, no. 11, pp. 6901–6910, 2021.

[8] R. Loureiro, S. Benmoussa, Y. Touati, R. Merzouki, and B. Ould Bouamama, "Integration of fault diagnosis and fault-tolerant control for health monitoring of a class of MIMO intelligent autonomous vehicles," *IEEE Trans. Veh. Technol.*, vol. 63, no. 1, pp. 30–39, 2014.

[9] Y. Fang, H. Min, W. Wang, Z. Xu, and X. Zhao, "A fault detection and diagnosis system for autonomous vehicles based on hybrid approaches," *IEEE Sensors J.*, vol. 20, no. 16, pp. 9359–9371, 2020.

[10] X. Cao, Y. Tian, X. Ji, and B. Qiu, "Fault-tolerant controller design for path following of the autonomous vehicle under the faults in braking actuators," *IEEE Trans. Transp. Elect.*, vol. 7, no. 4, pp. 530–540, 2021.

[11] A.-T. Nguyen, T.-M. Guerra, C. Sentouh, and H. Zhang, "Unknown input observers for simultaneous estimation of vehicle dynamics and driver torque: Theoretical design and hardware experiments," *IEEE/ASME Trans. Mechatron.*, vol. 24, no. 6, pp. 2508–2518, Dec. 2019.

[12] R. Rajamani, *Vehicle Dynamics and Control*. Springer US, 2012.

[13] B. Zhang, H. Du, J. Lam, N. Zhang, and W. Li, "A novel observer design for simultaneous estimation of vehicle steering angle and sideslip angle," *IEEE Trans. Indus. Electron.*, vol. 63, no. 7, pp. 4357–4366, 2016.

[14] A.-T. Nguyen, T. Dinh, T.-M. Guerra, and J. Pan, "Takagi–Sugeno fuzzy unknown input observers to estimate nonlinear dynamics of autonomous ground vehicles: Theory and real-time verification," *IEEE/ASME Trans. Mechatron.*, vol. 26, no. 3, pp. 1328–1338, 2021.

[15] T. Chen, L. Chen, X. Xu, Y. Cai, H. Jiang, and X. Sun, "Passive fault-tolerant path following control of autonomous distributed drive electric vehicle considering steering system fault," *Mech. Syst. Signal Process.*, vol. 123, pp. 298–315, 2019.

[16] J. Guo, J. Wang, Y. Luo, and K. Li, "Robust lateral control of autonomous four-wheel independent drive electric vehicles considering the roll effects and actuator faults," *Mech. Syst. Signal Process.*, vol. 143, p. 106773, 2020.

[17] S.-Y. Han, J. Zhou, Y.-H. Chen, Y.-F. Zhang, G.-Y. Tang, and L. Wang, "Active fault-tolerant control for discrete vehicle active suspension via reduced-order observer," *IEEE Trans. Syst., Man, Cybern.: Syst.*, vol. 51, no. 11, pp. 6701–6711, 2021.

[18] R. Sakthivel, S. Mohanapriya, C.-K. Ahn, and P. Selvaraj, "State estimation and dissipative-based control design for vehicle lateral dynamics with probabilistic faults," *IEEE Trans. Indus. Electron.*, vol. 65, no. 9, pp. 7193–7201, 2018.

[19] K. Lee and M. Lee, "Fault-tolerant stability control for independent four-wheel drive electric vehicle under actuator fault conditions," *IEEE Access*, vol. 8, pp. 91 368–91 378, 2020.

[20] M. Muenchhof, M. Beck, and R. Isermann, "Fault-tolerant actuators and drives–Structures, fault detection principles and applications," *Annu. Rev. Control*, vol. 33, no. 2, pp. 136–148, 2009.

[21] S. Ding, *Model-Based Fault Diagnosis Techniques: Design Schemes, Algorithms, and Tools*. Springer Science & Business Media, 2008.

[22] X. Dai and Z. Gao, "From model, signal to knowledge: A data-driven perspective of fault detection and diagnosis," *IEEE Trans. Indus. Inform.*, vol. 9, no. 4, pp. 2226–2238, 2013.

[23] I. Hwang, S. Kim, Y. Kim, and C. E. Seah, "A survey of fault detection, isolation, and reconfiguration methods," *IEEE Trans. Control Syst. Technol.*, vol. 18, no. 3, pp. 636–653, 2010.

[24] Z. Gao, C. Cecati, and S. Ding, "A survey of fault diagnosis and fault-tolerant techniques–Part I: Fault diagnosis with model-based and signal-based approaches," *IEEE Trans. Indus. Electron.*, vol. 62, no. 6, pp. 3757–3767, 2015.

[25] M. Chadli, A. Abdo, and S. Ding, "$\mathscr{H}_\infty/\mathscr{H}_-$ fault detection filter design for discrete-time Takagi–Sugeno fuzzy system," *Automatica*, vol. 49, no. 7, pp. 1996–2005, 2013.

[26] J. Li, Z. Wang, C.-K. Ahn, and Y. Shen, "Fault detection for Lipschitz nonlinear systems with restricted frequency-domain specifications," *IEEE Trans. Syst., Man, Cybern.: Syst.*, vol. 5, no. 2, pp. 486–496, 2021.

[27] J. Wang, G.-H. Yang, and J. Liu, "An LMI approach to $\mathscr{H}_-$ index and mixed $\mathscr{H}_-/\mathscr{H}_\infty$ fault detection observer design," *Automatica*, vol. 43, no. 9, pp. 1656–1665, 2007.

[28] C.-Z. Liu, L. Li, J.-W. Yong, F. Muhammad, and S. Cheng, "An innovative finite frequency $\mathscr{H}_\infty$ observer for Radar tracking," *IEEE Trans. Intell. Transp. Syst.*, vol. 22, no. 3, pp. 1553–1561, 2021.

[29] H. Zhang and J. Wang, "Active steering actuator fault detection for an automatically-steered electric ground vehicle," *IEEE Trans. Veh. Technol.*, vol. 66, no. 5, pp. 3685–3702, 2017.

[30] S. Wang, J. Pan, A.-T. Nguyen, T.-M. Guerra, and J. Lauber, "Takagi-Sugeno fuzzy fault detector design with finite-frequency specifications for autonomous ground vehicles," *IFAC-PapersOnLine*, vol. 54, no. 4, pp. 195–200, 2021.

[31] K. Zhang, B. Jiang, and V. Cocquempot, "Fuzzy unknown input observer-based robust fault estimation design for discrete-time fuzzy systems," *Signal Process.*, vol. 128, pp. 40–47, 2016.

[32] M. Zhou, Z. Cao, M. Zhou, and J. Wang, "Finite-frequency $\mathscr{H}_-/\mathscr{H}_\infty$ fault detection for discrete-time T–S fuzzy systems with unmeasurable premise variables," *IEEE Trans. Cybern.*, vol. 51, no. 6, pp. 17–26, 2021.

[33] T. Iwasaki and S. Hara, "Generalized KYP lemma: Unified frequency domain inequalities with design applications," *IEEE Trans. Autom. Control*, vol. 50, no. 1, pp. 41–59, 2005.

[34] Z. Wang, P. Shi, and C.-C. Lim, "$\mathscr{H}_-/\mathscr{H}_\infty$ fault detection observer in finite frequency domain for linear parameter-varying descriptor systems," *Automatica*, vol. 86, pp. 38–45, 2017.

[35] X.-J. Li and G.-H. Yang, "Fault detection in finite frequency domain for takagi-sugeno fuzzy systems with sensor faults," *IEEE Trans. Cybern.*, vol. 44, no. 8, pp. 1446–1458, 2013.

[36] K. Zhang, B. Jiang, P. Shi, and J. Xu, "Analysis and design of robust $\mathscr{H}_\infty$ fault estimation observer with finite-frequency specifications for discrete-time fuzzy systems," *IEEE Trans. Cybern.*, vol. 45, no. 7, pp. 1225–1235, 2015.

[37] R. Wang, H. Jing, H. Karimi, and N. Chen, "Robust fault-tolerant $\mathscr{H}_\infty$ control of active suspension systems with finite-frequency constraint," *Mech. Syst. Signal Process.*, vol. 62, pp. 341–355, 2015.

[38] X. Lu, Z. Liu, J. Zhang, H. Wang, Y. Song, and F. Duan, "Prior-information-based finite-frequency $\mathscr{H}_\infty$ control for active double pantograph in high-speed railway," *IEEE Trans. Veh. Technol.*, vol. 66, no. 10, pp. 8723–8733, 2017.
[39] J. Pan, A.-T. Nguyen, T.-M. Guerra, and D. Ichalal, "A unified framework for asymptotic observer design of fuzzy systems with unmeasurable premise variables," *IEEE Trans. Fuzzy Syst.*, vol. 29, no. 10, pp. 2938–2948, 2021.
[40] K. Tanaka and H. Wang, *Fuzzy Control Systems Design and Analysis: a Linear Matrix Inequality Approach*. NY: Wiley-Interscience, 2004.
[41] A.-T. Nguyen, T. Taniguchi, L. Eciolaza, V. Campos, R. Palhares, and M. Sugeno, "Fuzzy control systems: Past, present and future," *IEEE Comput. Intell. Mag.*, vol. 14, no. 1, pp. 56–68, Feb. 2019.
[42] A.-T. Nguyen, C. Sentouh, and J.-C. Popieul, "Driver-automation cooperative approach for shared steering control under multiple system constraints: Design and experiments," *IEEE Trans. Indus. Electron.*, vol. 64, no. 5, pp. 3819–3830, May 2017.
[43] P. Coutinho, R. Araújo, A.-T. Nguyen, and R. Palhares, "A multiple parameterization approach for local stabilization of constrained Takagi-Sugeno fuzzy systems with nonlinear consequents," *Inf. Sci.*, vol. 506, pp. 295–307, Jan. 2020.
[44] H. Trinh and T. Fernando, *Functional Observers for Dynamical Systems*. Springer Science & Business Media, 2011, vol. 420.
[45] G. Phanomchoeng and R. Rajamani, "The bounded Jacobian approach to nonlinear observer design," in *American Control Conference*, Baltimore, USA, July 2010, pp. 6083–6088.
[46] M. De Oliveira, J. Bernussou, and J. Geromel, "A new discrete-time robust stability condition," *Syst. Control Lett.*, vol. 37, no. 4, pp. 261–265, 1999.
[47] J. Löfberg, "Yalmip: A toolbox for modeling and optimization in Matlab," in *IEEE Int. Symp. Comput. Aided Control Syst. Des.*, Taipei, Sept. 2004, pp. 284–289.

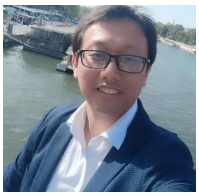

Juntao Pan received the B.Sc. degree in communication engineering and M.Sc. degree in control theory and control engineering from Three Gorges University, Yichang, China, in 2006 and 2008, respectively, and the Ph.D. degree in control theory and control engineering from Southeast University, Nanjing, China, in 2012.

He is currently an Associate Professor with North Minzu University, Yinchuan, China. His current research interests include fuzzy control, robust control, nonlinear control and their applications.

Anh-Tu Nguyen (M'18, SM'21) is an Associate Professor at the INSA Hauts-de-France, Université Polytechnique Hauts-de-France, Valenciennes, France. He received the degree in engineering and the M.Sc. degree in automatic control from Grenoble Institute of Technology, Grenoble, France, in 2009, and the Ph.D. degree in automatic control from the University of Valenciennes, Valenciennes, France, in 2013. He is an Associate Editor for the IEEE Transactions on Intelligent Transportation Systems, the IFAC journal Control Engineering Practice, the IET Journal of Engineering, the SAE International Journal of Vehicle Dynamics, Stability, and NVH, the Springer Automotive Innovation, Frontiers in Control Engineering, and a Guest Editor for special issues in various international journals. His research interests include robust control and estimation, cybernetics control systems, human-machine shared control with a strong emphasis on mechatronics applications.

Thierry-Marie Guerra is a Full Professor at the Polytechnic University Hauts-de-France, Valenciennes, France. He received his PhD degree in automatic control in 1991 and the HDR in 1999. From 2009 to 2019, he was head of the Laboratory of Industrial and Human Automation, Mechanics and Computer Science (LAMIH CNRS UMR 8201) (148 researchers and staff, 110 PhD students and postdocs) http://www.univ-valenciennes.fr/LAMIH/. He is chair of the Technical Committee 3.2 "Computational Intelligence in Control" for IFAC, member of the IFAC TC 7.1 "Automotive Control", Area Editor of the international journals: Fuzzy Sets & Systems and IEEE Transactions on Fuzzy Systems. His research fields and topics of interest are wine, hard rock, stamps, nonlinear control, LPV, Takagi-Sugeno models control and observation, LMI constraints, nonquadratic Lyapunov functions and applications to mobility, soft robotics and disabled persons.

Chouki Sentouh received the M.Sc. degree from the University of Versailles, Versailles, France, in 2003, and the PhD degree in automatic control from the University of Évry, Évry, France, in 2007.

He was a postdoctoral researcher at the laboratory IRCCyN UMR CNRS 6597, Nantes, France, from 2007 to 2009. Since 2009, he is an Associate Professor at the University of Valenciennes, laboratory LAMIH UMR CNRS 8201, Valenciennes, France. His research fields include automotive control, driver assistance systems with driver interaction, human driver modeling and cooperation in intelligent transportation systems. He is interested in shared control approaches to design assistance systems that can adapt their behavior according to the level of automation and the interaction with human driver.

Sujun Wang received his B.Sc. degree in Automation from North Minzu University, Ningxia, China, in 2018. He is currently a M.Sc. student at the North Minzu University, Ningxia, China. His current research interests include fuzzy control and applications.

Jean-Christophe Popieul received the Ph.D. in automatic control from the University of Valenciennes, Valenciennes, France, in 1994. He is a Professor of automatic control with the same university, laboratory LAMIH UMR CNRS 8201, Valenciennes, France. His research interests include transport safety, driver status assessment, shared control for full driving automation. Prof. Popieul is a member of several scientific boards, including ANR, PREDIT, i-Trans competitivity cluster, IRT Railenium. He is also the Head of several Interactive Simulation Platforms of the LAMIH: the SHERPA driving simulator, the PSCHITT-Rail train/tramway simulator, and the PSCHITT-PMR wheelchair simulator.